Toward soliton emission in asymmetric GaAs/AlGaAs multiple-quantum-well waveguide structures below the half-bandgap

Patrick Dumais and Alain Villeneuve

Pavillon Vachon, Université Laval, Cité Universitaire, Quebec G1K 7P4, Canada

Amr Saher-Helmy and J. Stewart Aitchison

Department of Electronics and Electrical Engineering, University of Glasgow, Glasgow G12 8QQ, UK

Lars Friedrich, Russell A. Fuerst, and George I. Stegeman

Center for Research and Education in Optics and Lasers, University of Central Florida, P.O. Box 162700, Orlando, Florida 32816-2700

Received March 2, 2000

We report what is to our knowledge the first experimental evidence of nonlinear beam displacement in a strip-loaded GaAs/AlGaAs multiple-quantum-well waveguide with an asymmetric, nonlinear cladding. An intensity-dependent spatial displacement of $\sim 2\ \mu$m was observed for the guided mode at a wavelength of 1.55 μm. Numerical simulations that correspond to the experiment are also presented. The device has the potential of providing a soliton-emission-based, ultrafast all-optical switch. © 2000 Optical Society of America

OCIS codes: 190.4420, 190.4390, 190.4360, 190.4310, 190.5970.

Nonlinear transverse field effects have been predicted and studied continually since Kaplan published his research on refraction upon a nonlinear interface.[1,2] The nonlinear interface is typically located between a linear medium and a nonlinear (Kerr) medium that exhibits an intensity-dependent refractive index. The initial study and a subsequent analysis involving Gaussian beams[3] predicted jumps in the reflectivity on such an interface that were later observed experimentally with a glass–CS_2 interface.[4] The proof of principle of nonlinear refraction was thus presented with a large, resonant nonlinearity. Generalizing the two-medium nonlinear refraction to multilayers introduced the new field of nonlinear guided waves. Extensive analysis[5–8] yielded analytical solutions of the so-called nonlinear modes of these structures. Foreseen applications[9] were optical limiting, optical thresholding, and optical switching. The stability of the analytical solutions in propagation was later studied.[10,11] This study led to that of the propagation of field distributions that were not solutions of the nonlinear Schrödinger equation,[12] followed by the purely numerical study of nonlinear wave propagation in these structures.[13,14] This did not, however, prevent other analytical studies and new approaches[15–18] from being pursued. One interesting phenomenon that did emerge from the study of the nonlinear slab waveguide is the emission of the spatial soliton.[19] In this situation, the waveguide is typically a linear slab waveguide clad with a nonlinear medium on one side and with a linear medium on the other. For a given input power, the guided wave would switch into the nonlinear cladding. It must be remarked that few corresponding experimental studies have emerged over the past decades. Experiments that involve nonlinear waveguides are limited to the observation of a saturation in transmissivity,[20] again by use of a large, resonant nonlinearity.

In this Letter we describe the experimental study of a nonlinear waveguide that relies on a bound electronic (or nonresonant) nonlinearity. Although we did not observe the emission of a soliton, we did observe evidence of a nonlinear transverse effect. This would be, to our knowledge, the first experimental observation of a transverse effect in a nonlinear waveguide by use of a nonresonant nonlinearity.

The waveguide (see Fig. 1) is an AlGaAs strip-loaded channel waveguide. The guiding layer is a multiple-quantum-well (MQW) structure. To produce the nonlinear cladding in this structure we disordered the MQW layer locally everywhere but in one of the cladding regions. Inasmuch as disordering lowers the n_2 coefficient, this altered cladding then becomes the nonlinear cladding. This recent development in superlattice processing has experimentally

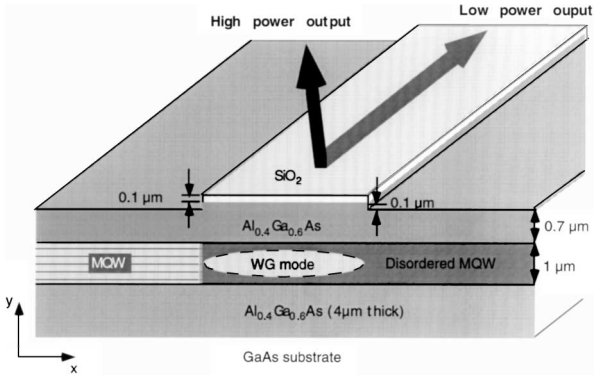

Fig. 1. Waveguide and device structures: WG, waveguide.

0146-9592/00/171282-03$15.00/0

demonstrated a decrease of 64% in the n_2 coefficient after disordering.[21]

The waveguide is single mode in the 1.55-μm spectral region. This wavelength is below the half-bandgap of the MQW waveguide material, so two-photon absorption is minimized. The wafer structure was grown upon a SI GaAs substrate, as illustrated in Fig. 1. The MQW region consists of 76 periods of 2.8-nm GaAs wells with 10-nm $Al_{0.4}Ga_{0.6}As$ barriers. We define the waveguide by strip-loading the structure with 200 nm of SiO_2 and etching 100 nm off the top AlGaAs layer on each side of the strip. Disordering is achieved through an impurity-free vacancy-disordering technique[21] in which dielectric caps are used during rapid thermal annealing to control the outdiffusion of Ga from the semiconductor. Ga outdiffusion has a substantial effect on the interdiffusion rates of Al and Ga across the MQW heterostructures. The sample presented here used SiO_2 and SiO_2:P, respectively, to enhance and inhibit intermixing. Standard photolithography was used for patterning these dielectric caps. The losses measured for an undisordered waveguide on the same wafer were of the order of 1.4 dB/cm. Because disordering increased scattering, typically doubles the losses, we estimate a loss of 3 dB/cm for the intermixed device.

A line-buildout-based optical parametric generated–optical parametric amplifier system pumped by a Q-switched, frequency-doubled YAG laser was used for testing the 3-mm-long sample. The output pulses had energies of the order of 10 μJ with pulse widths of 20 ps at a repetition rate of 10 Hz and a wavelength of 1560 nm. A 40× microscope objective was used to couple-in a collimated beam of 2.5-mm diameter, which produced a 1.6-μm spot. The corresponding Rayleigh length for this setup is ~5 μm. The mode size of the waveguide was 10 μm × 0.8 μm. The intensity overlap between the mode and the Gaussian input beam was ~0.3. The beam had to be slightly decoupled into the waveguide to prevent optically induced damage. The fluence at the focal point was sufficiently large to induce optical damage within the waveguide or at the surface. In view of the overlap integral and reflection losses, the maximum coupled peak power was 25 kW, corresponding to a peak intensity of 200 GW/cm^2, which is the upper limit for this setup. For these conditions we observed an intensity-dependent lateral shift of ~2 μm for a mode width of 10 μm. Line scans from the output face of the device, at high and low input peak intensities, are illustrated in Fig. 2. Each intensity profile is normalized to its peak intensities.

We reduce the modeling of the two-dimensional waveguide (Fig. 1) to a one-dimensional problem through the effective-index method.[22] This reduction is justified because the index step that defines the slab waveguide (along the y axis) is of the order of 10^{-2}, whereas the strip changes in the effective index of the slab on a much lesser scale, of the order of 10^{-4}. The propagation in the structure can be thus modeled through a one-dimensional beam-propagation method, from a nonlinear Schrödinger equation the form

$$\frac{\partial^2\psi(z,x)}{\partial x^2} - 2i\beta_0\frac{\partial\psi(z,x)}{\partial z} + \left[\beta^2(x) - {\beta_0}^2 + \frac{2{k_0}^2 n_0 n_2(x)}{T_{\text{eff}}}|\psi(x,z)|^2 - i\beta_0\alpha\right]\psi(z,x) = 0, \quad (1)$$

where $\psi^2(z,x)$ is the linear intensity, T_{eff} is the effective thickness of the film, and $\psi^2(z,x)/T_{\text{eff}}$ represents an effective intensity. $n_2(x)$ is the Kerr coefficient (in square meters per watt), α is the linear loss, and $\beta(x)$ is the propagation constant of the slab waveguide (along the y axis) for a given lateral position (x). Thus $\beta(x)/k_0$ is the effective refractive index profile of the channel waveguide. β_0 is a propagation constant of arbitrary value (which must be close to any given value of $\beta(x)$] that we set to the lowest propagation constant of the effective structure [$\min(\beta(x)$]. n_0 is similarly given the value of β_0/k_0.

We can explain the device's operation simply and accurately by studying the effective refractive indices at the nonlinear interface. In essence, if the waveguide boundary can be cancelled out by the nonlinear contribution to the (effective) refractive index, soliton emission will occur[23] as schematized in Fig. 1.

For modeling, we used known refractive indices for AlGaAs (the average effective index is near 3.24) (Ref. 24) and a value of 3 dB/cm for losses, as we mentioned above. A nominal n_2 of 3.3×10^{-13} cm^2/W as measured by Yang *et al.*[25] for the MQW layer was assumed, as well as a 64% decrease of this coefficient in the disordered section, as reported. The estimated refractive-index step is of 4.4×10^{-4}. With these values we estimate that the emission threshold corresponds to a peak input intensity of approximately 6 GW/cm^2 (effective intensity). For that intensity, the soliton will be emitted after a propagation distance of 2.6 mm and travel at an angle of 3.2 mrad to the axis of the waveguide. The output beam profiles for the near emission that occurs at lower intensities are presented in Fig. 3. From this figure we can see that a 2-μm shift of the beam's maximum occurs for an input (effective) intensity of 3.5 GW/cm^2. Note that these simulations were made for input intensities that are constant in time; i.e., pulse-breakup effects are not included. Introducing the time dependence in this case would broaden the output beam as it passed through intermediate peak input intensities that have

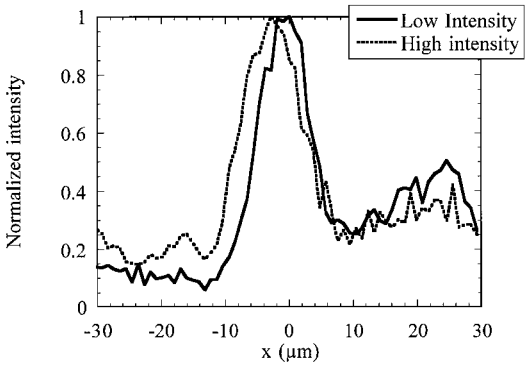

Fig. 2. Beam profiles at the device output face at low and high intensity.

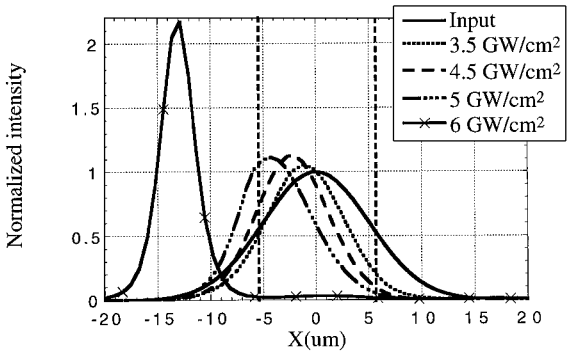

Fig. 3. Input and output profiles for several peak input intensities, illustrating the near-emission and the emission of a spatial soliton. The peak intensities given are effective intensities, represented by ψ^2/T_{eff} in Eq. (1).

distinct output profiles, as can be seen from Fig. 3. This simple decomposition would not be sufficient, however, to describe the case in which a soliton were emitted. Indeed, it has been shown numerically[26] that the emitted light undergoes some spatiotemporal clustering, which is attributed to modulational instability.

One fact that we neglected in the modeling presented here is that the disordering process introduces a refractive-index change. This change is estimated to be of the order of 10^{-3} (according to a simple model,[27] it would be 4×10^{-3} if complete intermixing were achieved). The refractive index increases with disordering. This increase will steepen the refractive-index step at the nonlinear interface of the waveguide, because the core index increases. The other interface is essentially unaffected because the linear cladding is modified in the same manner as is the core.

One effect of this steepening would be to increase the emission threshold. Although the threshold can be significantly increased, the effect on the device function is minor. Another effect of this one-sided steepening is to introduce an asymmetry in the mode profile. This asymmetry, conjoined with the Kerr effect, can lead to mode shape fluctuations that are independent of the n_2 step at the nonlinear interface. We cannot effectively rule out that the result presented in Fig. 2 is a mode transition of this nature. However, our simulations that include the estimated steepening (not shown) reveal that only the peak of the mode would shift, rather than there being a translation of the whole beam as in Fig. 2.

The effect of the waveguide boundary on soliton emission suggests an improved design for the waveguide that includes a well-defined input waveguide followed by a tapered section leading to a weakly guiding channel in which soliton emission could occur more easily. A curved waveguide can also produce this effect if it is curved away from the nonlinear cladding.

In conclusion, we have demonstrated experimentally a spatial nonlinear effect that is attributable to a spatially variant nonlinearity induced by the intermixing of a MQW layer. The experimental results are consistent with basic numerical simulations. The device has the potential of providing what may be the first soliton-emission-based, ultrafast all-optical switch.

The authors' e-mail addresses are pdumais@phy.ulaval.ca, avillene@phy.ulaval.ac.uk, a.saher@elec.gla.ac.uk, s.aitchison@elec.gla.ac.uk, lars@soliton.creol.ucf.edu, russell.fuerst.uniphase.com, and george@creol.ucf.edu.

References

1. A. E. Kaplan, JETP Lett. **24,** 114 (1976).
2. A. E. Kaplan, Sov. Phys. JETP **45,** 896 (1977).
3. W. J. Tomlinson, J. P. Gordon, P. W. Smith, and A. E. Kaplan, Appl. Opt. **21,** 2041 (1982).
4. P. W. Smith and W. J. Tomlinson, IEEE J. Quantum Electron. **QE-20,** 30 (1984).
5. N. N. Akhmediev, Sov. Phys. JETP **56,** 299 (1982).
6. G. I. Stegeman, C. T. Seaton, J. Chilwell, and S. D. Smith, Appl. Phys. Lett. **44,** 830 (1984).
7. U. Langbein, F. Lederer, and H.-E. Ponath, Opt. Commun. **53,** 417 (1985).
8. A. D. Boardman and P. Egan, IEEE J. Quantum Electron. **QE-21,** 1701 (1985).
9. C. T. Seaton, X. Mai, and G. I. Stegeman, Opt. Eng. **24,** 593 (1985).
10. C. K. R. T. Jones and J. V. Moloney, Phys. Lett. A **117,** 175 (1986).
11. J. V. Moloney, J. Ariyasu, C. T. Seaton, and G. I. Stegeman, Appl. Phys. Lett. **48,** 826 (1986).
12. C. T. Seaton, J. D. Valera, R. L. Shoemaker, G. I. Stegeman, J. T. Chilwell, and S. D. Smith, IEEE J. Quantum Electron. **QE-21,** 774 (1985).
13. L. Leine, C. Wächter, U. Langbein, and F. Lederer, J. Opt. Soc. Am. B **5,** 547 (1988).
14. D. Mihalache, D.-M. Baboiu, D. Mazilu, L. Torner, and J. P. Torres, J. Opt. Soc. Am. B **11,** 1244 (1994).
15. A. B. Aceves, P. Varatharajah, A. C. Newell, E. M. Wright, G. I. Stegeman, D. R. Heatley, J. V. Moloney, and H. Adachihara, J. Opt. Soc. Am. B **7,** 963 (1990).
16. N. Godbout and S. I. Najafi, Opt. Eng. **32,** 2064 (1993).
17. J. P. Torres and L. Torner, J. Opt. Soc. Am. B **11,** 45 (1994).
18. Y. S. Kivshar and M. L. Quiroga-Teixeiro, Phys. Rev. A **48,** 4750 (1993).
19. E. M. Wright, D. R. Heatley, and G. I. Stegeman, Phys. Rep. **194,** 309 (1990).
20. H. Vach, C. T. Seaton, and G. I. Stegeman, Opt. Lett. **9,** 238 (1984).
21. C. J. Hamilton, J. H. Marsh, D. C. Hutchings, J. S. Aitchison, G. T. Kennedy, and W. Sibbett, Appl. Phys. Lett. **68,** 3078 (1996).
22. D. Marcuse, *Theory of Dielectric Optical Waveguides*, 2nd ed. (Academic, San Diego, Calif., 1991), p. 330.
23. P. Dumais, A. Villeneuve, A. Saher-Helmy, and J. S. Aitchison, Opt. Express **2,** 455 (1998), http://epubs.osa.org/opticsexpress.
24. R. J. Deri and M. A. Emanuel, J. Appl. Phys. **77,** 4667 (1995).
25. C. C. Yang, A. Villeneuve, G. I. Stegeman, C.-H. Lin, and H.-H. Lin, IEEE J. Quantum Electron. **29,** 2934 (1993).
26. H. Michinel, Pure Appl. Opt. **6,** 537 (1997).
27. Y. Suzuki, H. Iwamura, T. Miyazawa, A. Wakatsuki, and O. Mikami, IEEE J. Quantum Electron. **32,** 1922 (1996).